Effect of Axial Fuel and Coolant Temperature Distribution in Homogenized Assembly Cross-Section Generation for a Boron-Free SMR Core

Hyo Yun Lee[1], Sung Hyun Cho[1], Woo Jin Lee[1], Ser Gi Hong[1]*
[1]Department of Nuclear Engineering, Hanyang University, 222 Wangsimni-ro, Seongdong-gu, Seoul 04763, Korea
*Corresponding author: hongsergi@hanyang.ac.kr

CT&RPL Computational Transport & Reactor Physics Laboratory HANYANG UNIVERSITY

Introduction

- **Background**
  - The soluble-boron-free SMR (Small Modular Reactor) core such as i-SMR uses the control rods as a main reactivity control mechanism in baseload and load-follow operations . This kind of control rod movement can result in the distortion of axial power distribution, leading to the distortion in the axial coolant and fuel temperature distribution.
  - Conventional two-step analysis depletes each fuel assembly at a single reference fuel/coolant temperature and generates branch cross sections only at selected burnup points.
  - These branch homogenized group constants (HGCs) may not preserve the axial temperature history accumulated during depletion.
- **Objective**
  - Quantify the changes in core calculation results caused by accounting for axial fuel and coolant temperature conditions in the HGC generatiuon.
  - Comparing the critical regulating-bank position, axial offset (AO), 3-D peaking factor (F_q), and radial peaking factor (F_r) over three fuel cycles.

Methods

- **Analysis Codes**
  - DeCART2D v1.1 generated assembly HGCs using the ENDF/B-VII.1 library.
  - MASTER v4.0 performed three-dimensional nodal diffusion and depletion calculations with the SENM solver.
- **Core Model**
  - 180 MWth PWR-type SMR with 37 fuel assemblies and five assembly types with different U-235 enrichment, burnable-absorber loading, and GdN content.
  - UN–GdN burnable absorber rods reduce excess reactivity while retaining favorable thermal properties.
  - Three regulating banks (R1–R3) and three shutdown banks (S1–S3) are adopted.

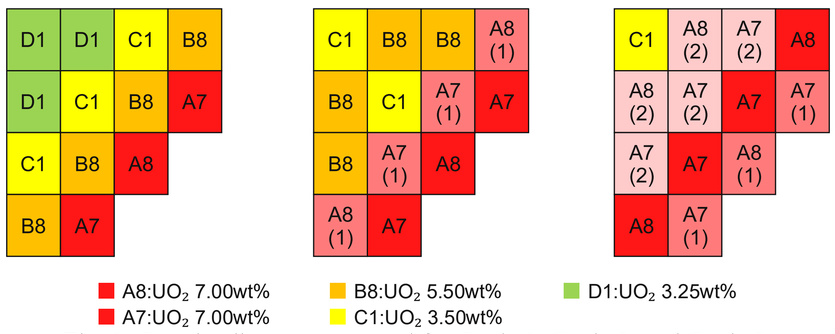


Fig. 1. Core loading patterns used for Cycle 1, Cycle 2, and Cycle 3.

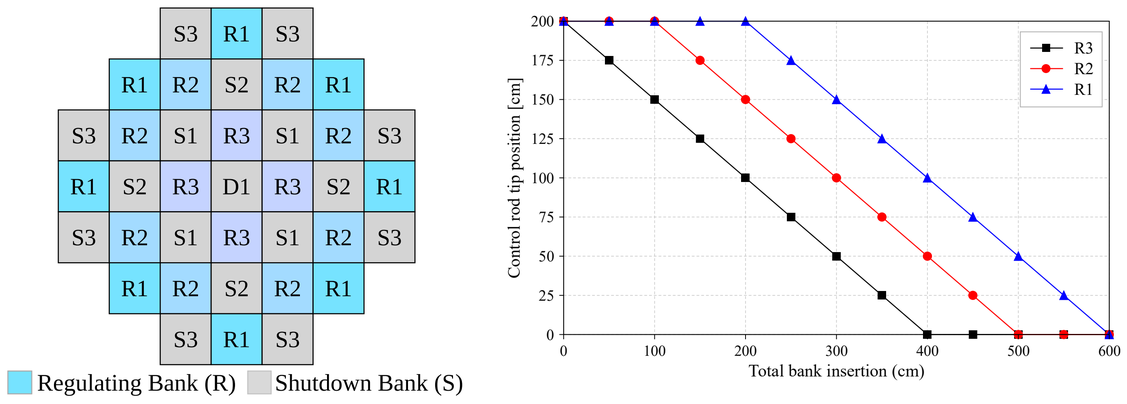


Fig. 2 Arrangement of control rods and Regulating bank insertion strategy

- **HGC Treatments**
  - Reference case (Case 1): Fuel and coolant temperature were fixed at reference temperature.
  - Axially temperature-dependent case (Case 2): The 200-cm active core height was divided into 20 axial nodes of 10 cm each. Separate lattice depletion calculations were performed using node-specific fuel and coolant temperatures to generate the HGC.

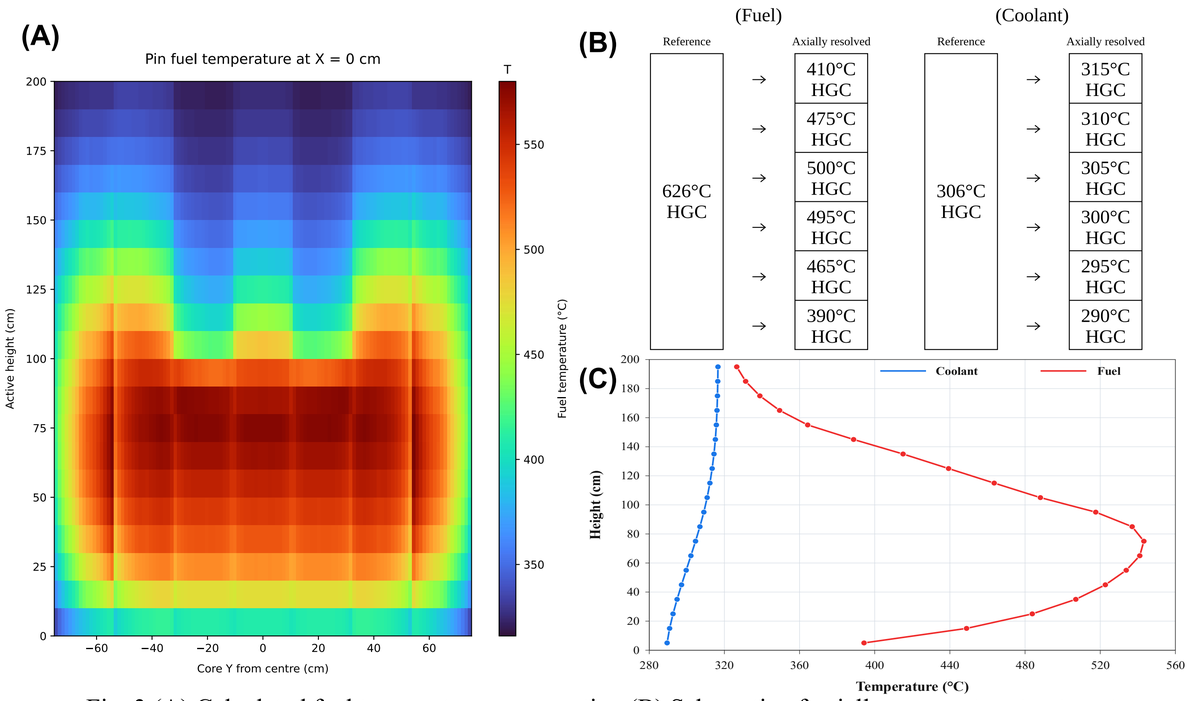


Fig. 3 (A) Calculated fuel temperature cross section (B) Schematic of axially temperature treatment (C) Averaged axial fuel and coolant temperature distribution

- **Axial Temperature Procedure**
  - Node-wise fuel and coolant temperatures were extracted and averaged from the 1st cycle of MASTER calculation.
  - The averaged node-wise axial temperature profiles were used to generate the HGCs applied in all cycles for axially temperature-dependent case.

Results and Discussion

- **Calculation Conditions**
  - Core geometry, loading pattern, depletion steps, and critical rod search method were identical in both cases.
  - All results were calculated under soluble-boron-free conditions. Differences were calculated from (axially temperature-dependent case - Reference case.)
- **The 1st cycle results**
  - Maximum absolute difference : 3.375 cm in regulating-bank position, 0.031 in AO, 0.168 in F_q, and 0.009 in F_r.

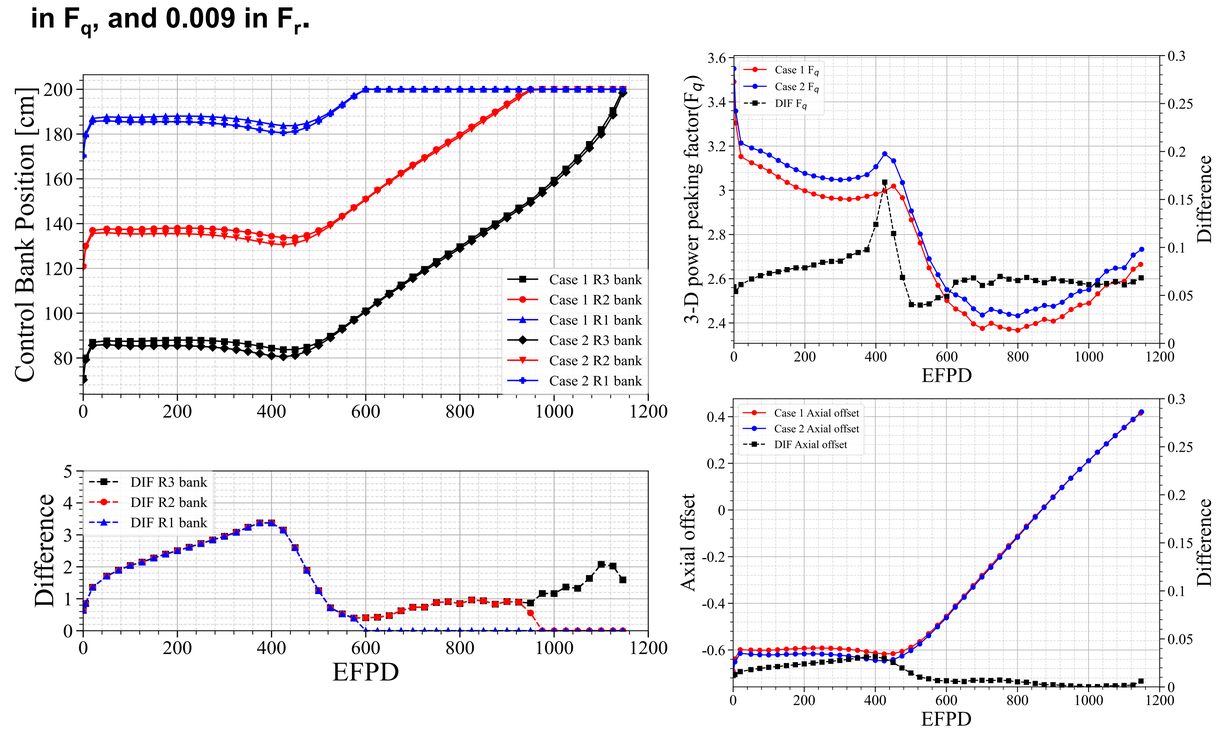


Fig. 4 Critical rod position of regulating bank, F_q, Axial offset as depletion for Cycle1

- **Cycle-Average Differences and Maximum Absolute Differences by Cycle**
  - Across Cycles 1–3, maximum difference : 5.894 cm in regulating-bank position, 0.031 in AO, 0.173 in F_q, and 0.038 in F_r.

Table 1. Cycle averaged and maximum absolute differences in critical rod position and power distribution

Critical rod position [cm]					3-D power peaking factor (F_q)				
Cycle	Case 1	Case 2	Avg. diff.	Max. diff.	Cycle	Case 1	Case 2	Avg. diff.	Max. diff.
CY01	167.826	166.693	-1.133	3.375	CY01	2.722	2.794	+0.072	0.168
CY02	151.046	150.175	-0.871	5.894	CY02	2.617	2.665	+0.048	0.173
CY03	158.702	158.264	-0.438	4.596	CY03	2.339	2.388	+0.049	0.121
Axial offset					**2-D power peaking factor (F_r)**				
Cycle	Case 1	Case 2	Avg. diff.	Max. diff.	Cycle	Case 1	Case 2	Avg. diff.	Max. diff.
CY01	-0.309	-0.320	-0.013	0.031	CY01	1.483	1.485	+0.003	0.009
CY02	-0.095	-0.108	-0.013	0.026	CY02	1.462	1.464	+0.002	0.010
CY03	-0.089	-0.100	-0.011	0.030	CY03	1.463	1.478	+0.015	0.038

- **Discussion**
  - Axial temperature-dependent treatment changed the node-wise HGC, changing flux and power and the regulating-bank position.
  - F_q and AO were more sensitive than F_r because the node-wise temperature was axially applied.
  - The 2nd cycle and the 3rd cycle exhibited smaller average rod-position differences than the 1st cycle, but their max absolute differences were larger.
  - In the 2nd and the 3rd cycle, the difference gradually increased from BOC to EOC. The difference reached its maximum at EOC.

Conclusions

- Fixed reference-temperature and axially temperature-dependent HGC treatments were compared in three-cycle, soluble-boron-free MASTER depletion calculations.
- The overall depletion results showed similar trend in both case, but the axially temperature-dependent treatment exhibited noticeable changes in critical rod position, AO, and power peaking.
- The results indicated that the temperature conditions used for HGC generation can affect the predicted control rod insertion history and local power distribution in soluble-boron-free cores.
- Such differences may significantly affect subsequent safety analysis results.
- In future work, applied axial temperature distribution will be updated iteratively through coupled lattice and core calculations.

Acknowledgment

This work was supported by the Korea Institute of Energy Technology Evaluation and Planning (KETEP) and the Ministry of Climate, Energy & Environment (MCEE) of the Republic of Korea. (No. RS-2024-00398867).

[1] H. O. Kang, B. J. Lee, and S. G. Lim, “Light Water SMR Development Status in Korea,” Nuclear Engineering and Design, Vol. 419, 112966, 2024.
[2] I. Bilodid and S. Mittag, “Use of the Local Pu-239 Concentration as an Indicator of Burnup Spectral History in DYN3D,” Annals of Nuclear Energy, Vol. 37, No. 9, pp. 1208–1213, 2010.
[3] S. T. Oh and S. G. Hong, “Effectiveness of UN-GdN Burnable Absorber for 180MWt SMR Core Loaded with LEU+ Fuels,” Transactions of the Korean Nuclear Society Spring Meeting, Jeju, Korea, May 7–8, 2026.
[4] J. Y. Cho, et al., “DeCART2D v1.1 User’s Manual,” KAERI/UM-40/2016, 2016.
[5] J. Y. Cho, et al., “MASTER v4.0 User’s Manual,” KAERI/UM-41/2016, 2016.